

# PyramidCLIP: Hierarchical Feature Alignment for Vision-language Model Pretraining

Yuting Gao<sup>1\*</sup> Jinfeng Liu<sup>1,2,\*</sup> Zihan Xu<sup>1,\*</sup> Jun Zhang<sup>1</sup> Ke Li<sup>1</sup> Chunhua Shen<sup>3</sup>

<sup>1</sup>Tencent Youtu Lab    <sup>2</sup>Shanghai Jiaotong University    <sup>3</sup>Zhejiang University  
 {yutinggao, ianxxu, bobbyjzhang, tristanli}@tencent.com

## Abstract

Large-scale vision-language pre-training has achieved promising results on downstream tasks. Existing methods highly rely on the assumption that the image-text pairs crawled from the Internet are in perfect one-to-one correspondence. However, in real scenarios, this assumption can be difficult to hold: the text description, obtained by crawling the affiliated metadata of the image, often suffer from *semantic mismatch* and *mutual compatibility*. To address these issues, here we introduce PyramidCLIP, which constructs an input pyramid with different semantic levels, and aligns visual elements and linguistic elements in the form of hierarchy via *intra-level semantics alignment* and *cross-level relation alignment*. Furthermore, we adjust the objective function by softening the loss of negative samples (unpaired samples) so as to weaken the strict constraint during the pre-training stage, thus mitigating the risk of the model being over-confident. Experiments on three downstream tasks, including zero-shot image classification, zero-shot image-text retrieval and image object detection, verify the effectiveness of the proposed PyramidCLIP. In particular, with the same amount of pre-training data of 15 millions image-text pairs, PyramidCLIP exceeds CLIP by 19.2%/18.5%/19.6% respectively, with the image encoder being ResNet-50/ViT-B32/ViT-B16 on ImageNet zero-shot classification top-1 accuracy. When scaling to larger datasets, the results of PyramidCLIP only trained for 8 epochs using 128M image-text pairs are very close to that of CLIP trained for 32 epochs using 400M training data.

## 1 Introduction

Recently, vision-language pre-training (VLP) has shown great success, which aims to improve the accuracy of downstream vision-language tasks by pre-training a model on large-scale image-text pairs harvested from the web without any manual annotation. The mainstream VLP methods can be roughly categorized into two paradigms, single-stream [1, 2, 3, 4, 5] and dual-stream [6, 7, 8, 9]. Compared to the single-stream counterpart, the dual-stream paradigm decouples the image encoder and text encoder and extracts features for image and text respectively, making the dual-stream paradigm more friendly for downstream applications. Due to the advantages of performance and efficiency, the dual-stream paradigm dominates. CLIP [6] preforms contrastive image-language pre-training on 400M image-text pairs collected from the Internet, which achieves astounding results. Later, methods such as DeCLIP [10] and FILIP [8] improve CLIP by introducing self-supervision in the image modal and text modal, and bringing in more fine-grained alignment on ViT [11] patch tokens.

Although existing CLIP-alike methods have achieved very promising results on downstream tasks, they strongly rely on the assumption that the image-text pairs are of high quality: the image and text are of good matching. Ideally, the pairs are in perfect one-to-one correspondence and have

\*The first three authors contributed equally. This work was done when J. Liu was an intern at Tencent.



**Figure 1: Problems in the web-crawled image-text pairs.** (a)(b) and (c) suffer the semantic mismatch between the visual modality and the linguistic modality, while the image-text of (d) has similarities with the unpaired text-image of (a). Note that, (a) the red caption is redundant, (b) the image outside the red bounding box is the redundant, (c) the descriptions for the casts in the red boxes are missing and the red caption in (d) is compatible with (a).

no correlation with other unpaired samples. However, in practice this assumption is not easy to satisfy as shown in Figure 1. Firstly, semantic mismatch between the visual modality and linguistic modality often exists within image-text pairs, *e.g.*, (a) Caption Redundancy: text describes too much redundant and fine-grained details while image needs a more concise caption; (b) Image Redundancy: a Region-of-Interest (ROI) corresponding to the text is only a sub-region of the image; and (c) Cast Deficiency: text misses the descriptions of salient objects in the image, while visual modeling needs to reason about the relationship among instances. Besides, Mutual Compatibility (d) usually occurs among pairs, *i.e.*, pairs have more or less local similarities. For example, the image/text of (d) can partially correspond to the text/image of (a). However, existing approaches directly treat other pairs as negative samples regardless the correlation, which can lead the model to overfit.

In order to tackle the issues mentioned above, we propose **PyramidCLIP** in this paper, which attempts to align image and text more precisely in the form of hierarchy. PyramidCLIP constructs an input pyramid with different semantic levels at both sides of the dual-stream network, *i.e.*, the global image, local image regions, and features of the salient instances in the image for visual modeling; the original caption and text summarization for linguistic modeling. Then we contrast visual elements and linguistic elements via *intra-level semantics alignment* and *cross-level relation alignment*, tackling the issues of (a)(b) and (c) respectively. Specifically, for intra-level semantics alignment, since the global region of the image and text summarization both contain global semantic information, while the local region and original caption both contain more fine-grained semantic information, thus they are treated as two pairs of positive samples. For cross-level relation alignment, to avoid the visual encoder’s modelling of the object relationship being overwhelmed by the scene semantics modelling, we explicitly align the instance relation with linguistic elements. Moreover, for the issue of Mutual Compatibility, we soften the loss term of the negative unpaired samples during the contrast process to ease the strict constraint, alleviating the negative effect of some local similarities.

Extensive experiments demonstrate the effectiveness of our proposed PyramidCLIP. For fair comparison, when trained with the YFCC15M [12] dataset, with ResNet-50 [13]/ViT-B32 [11]/ViT-B16 [11] as the image encoder and Transformer as the text encoder, our model achieves the state-of-the-art (SoTA) zero-shot classification on ImageNet [14], namely, 44.7%/41.4%/47.2% top-1 accuracy. In comparison, the CLIP baseline is 22.5%/22.9%/27.6%. Furthermore, when scaling to larger-scale dataset, the results of PyramidCLIP only trained for 8 epochs on 128M image-text pairs are very close to that of CLIP trained for 32 epochs on a 400M dataset, significantly improving the training and data efficiency of CLIP.

Our main contributions are summarized as follows:

- We propose PyramidCLIP for more accurate image-text alignment for vision-language model pre-training, which effectively constructs an input pyramid at both sides of the visual encoder and linguistic encoder, and then align the visual elements and linguistic elements via intra-level semantic alignment and cross-level relation alignment.
- We soften the loss term of negative samples during the contrast process to ease the strict constraint, so as to avoid the model being over-confident, alleviating the negative effect caused by local similarities.
- Extensive experiments demonstrate the effectiveness of PyramidCLIP. In the case of the same amount of pre-training data, PyramidCLIP achieves SoTA results, and significantly outperforms that of CLIP.

## 2 Related Work

**Vision-Language Pre-training** Vision-Language Pre-training (VLP) learns a strong joint representation between two modalities by pre-training models on large-scale image-text pairs, and it shows impressive transferability on a few downstream vision and language tasks. In terms of the model architecture design, the mainstream VLP models can be divided into two types: single-stream (early fusion of the two input modalities) and dual-stream (late fusion). The former one uses a single transformer to model both image and text representations in a unified semantic space by concatenating image and text input embeddings, including VisualBERT [2], UNITER [1], UNICODER [4], OSCAR [3] and UNIMO [15]. While the latter one encodes images and texts separately with a decoupled image encoder and a text encoder for high-level representations, such as ViLBERT [16], LXMERT [9], ALIGN [7], CLIP [6], and DeCLIP [10]. From a different perspective, the pre-training objective mainly comprises two categories: image-text contrastive learning and masked token tasks based on Language Modeling (LM). Among the methods mentioned above, UNIMO, ALIGN, CLIP and DeCLIP adopt contrastive learning to pull closer positive samples while pushing away negative samples. In contrast, VisualBERT, UNITER, LXMERT, UNICODER use masked token tasks, including Masked Language/Region Modeling and autoregressive LM. In this paper, we employ the dual-stream architecture and contrastive learning for simplicity, flexibility, and relatively cheaper computation.

**Fine-grained Alignment** Due to the semantic gap between image and text, there may be some troubles in directly performing the alignment between these two modalities. For example, the corresponding descriptions of the objects in an image are not always available in the caption. On the other hand, some words or phrases in the descriptions may be irrelevant to the images. Thus, finer-grained alignment is indispensable, as it can reduce noises and provide more accurate, richer supervision signals of multiple granularity, thus significantly improving the training efficiency and model performance. FILIP [8] improves the contrastive objective to achieve finer-level alignment, by using a token-wise maximum similarity between visual and textual tokens. While other methods [3, 17, 18, 19] construct multi-level semantic concepts for finer-grained alignment. OSCAR [3] first introduces multi-level semantics, captures object region features and the corresponding tags with a pre-trained object detector, then concatenates text, object tags and region features to learn the joint representations. VinVL [17] enhances the visual representations of OSCAR by pre-training a more powerful object detector. Both OSCAR and VinVL form the multi-level semantics only in the visual modality. MVPTR [18] and X-VLM [19] obtain their multi-level semantics concepts in both visual and linguistic modalities. MVPTR limits the interaction between object tags and textual tokens, learns the object-tag alignment in an explicit manner, and also models the nested property of language by learning phrase-level semantics. X-VLM learns multi-level alignments by positioning vision concepts using given texts, and makes alignments between these two parts. However, in addition to the image encoder and the text encoder, the two methods both have an additional cross-modal encoder, introducing computation overhead.

In this paper, we follow the dual-stream design from CLIP and construct three visual semantics levels and two linguistic semantics levels to form our PyramidCLIP. Different from methods mentioned above, each level is input to the corresponding encoder individually, without concatenating. The obtained three visual representations and two linguistic representations are used to compute four contrastive loss terms, which helps to achieve multi-level alignments.

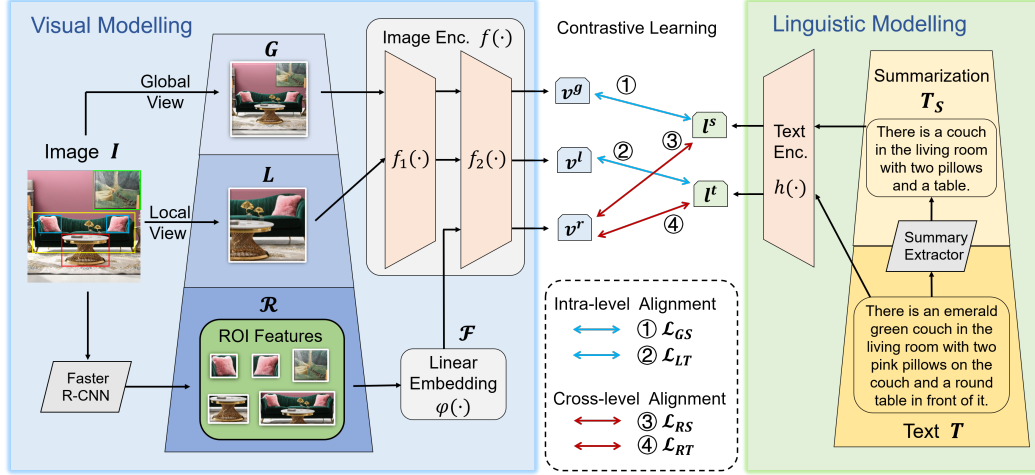


**Figure 2: The overall architecture of the proposed PyramidCLIP which is a dual-stream network.** The input elements of visual modelling is of three-level semantics, and the linguistic modelling has two-level semantics inputs. The elements of the two modalities interact through intra-level semantics alignment and cross-level relation alignment.

### 3 Method

In this section, we introduce the proposed PyramidCLIP for more accurate alignment of image and text for vision-language model pre-training. We first present the overall architecture in Section 3.1, and then introduce *intra-level semantics alignment* and *cross-level relation alignment* in detail in Section 3.2 and Section 3.3. Finally, the softened objective function is described in Section 3.4.

#### 3.1 Overall Architecture

The entire framework of the proposed PyramidCLIP is presented in Figure 2. PyramidCLIP is a dual-stream network, including a text encoder  $h$  and an image encoder  $f = f_2 \circ f_1$ , where  $f_1$  and  $f_2$  denote the front part and the rear part of the image encoder respectively. Each encoder consists of a linear projector and a normalization operator in the end to project the final class token into the unified dimension and then normalize it, obtaining the corresponding visual or linguistic representation vector in the same embedded space.

During the training, for each image-text pair  $(I, T)$ , the image  $I$  is transformed into two views, *i.e.*, local view  $L$  and global view  $G$ , through random crop with different ratios, and text  $T$  is input to a summary extractor [20] to generate text summarization  $T_S$  with higher level semantics. The image global view  $G$  and text summarization  $T_S$  both capture more global context information, while the image local view  $L$  and original text  $T$  contain more detailed information. Therefore,  $G$  and  $T_S$  are regarded as a pair of positive samples, while  $L$  and  $T$  are regarded as another pair of positive samples, denoted as  $(G, T_S)$  and  $(L, T)$ . Then these two pairs are input to the dual-stream encoder to extract global and local representation pairs,  $(v^g, l^s)$  and  $(v^l, l^t)$ , where  $v^g = f(G)$ ,  $l^s = h(T_S)$ ,  $v^l = f(L)$  and  $l^t = h(T)$ . Finally,  $(v^g, l^s)$  and  $(v^l, l^t)$  are pulled together through contrastive learning loss ① and ② respectively (refer to Figure 2), and other samples in the same batch are treated as negative samples. We term this contrasting process as *Intra-level Semantics Alignment*.

Furthermore, in order to explicitly model the relationship between salient objects in the image, the ROI feature sequences  $\mathcal{R} = \{o_1, o_2, \dots, o_M\}$  of  $M$  detected salient objects in the image  $I$  are extracted through a pre-trained object detector Faster R-CNN [21]. Then a linear embedding module  $\varphi$  is used to transform the ROI feature sequence  $\mathcal{R}$  into the same dimension as the output of the front part  $f_1$  of the image encoder. The sequence is successively fed into the rear part  $f_2$ , which contains one or more Multi-head Self-attention (MHSA) layers [11], to adaptively capture the relation between these salient instances, generating the final representation vector  $v^r$ , *i.e.*,  $v^r = f_2(\varphi(\mathcal{R}))$ . To avoid the visual model’s modelling of relation being overwhelmed by the context semantic modelling and weakening the ability of reasoning, we have  $(v^r, l^s)$  and  $(v^r, l^t)$  as another two positive pairs, and

the distance between ROI embedding and corresponding language embedding are being narrowed through contrastive learning loss ③ and ④, termed as *Cross-level Relation Alignment*.

It is worth noting that at the inference stage, only the original image-text pair  $(I, T)$  is used, *i.e.*, the visual representation  $v^i$  from  $I$  and the linguistic representation  $l^t$  from  $T$ .

### 3.2 Intra-level Semantics Alignment

Now we present the details of the intra-level semantics alignment. As mentioned above, the dual-stream vision-language contrastive learning methods such as CLIP strongly rely on that the image-text pairs are of good quality of one-to-one correspondence. However, semantic mismatch between images and text captions often occurs in the automatically harvested data. Therefore, we construct an input pyramid with multi-level semantics on both sides of the dual-stream network, and then align image and text within the same semantics level. Specifically, the image  $I$  is transformed to the global view  $G$  and the local view  $L$  through two random crops with different ratios. For the text caption, besides the original caption  $T$ , text summarization  $T_S$  with more compact semantics is extracted using a pre-trained text summarization extractor.

**Coarse-grained Global Contrast** We set the random crop ratio for generating global view  $G$  to be  $[0.9, 1]$ , which basically contains all the information in the original image. Text summarization  $T_S$  condenses the original caption  $T$ , removing some redundant and overly detailed information in the  $T$ .  $G$  and  $T_S$  both capture global information and can be used as pairs of positive samples. The projected embedding  $v^g$  and  $l^s$  of  $G$  and  $T_S$  are pulled closer through contrastive learning.

**Fine-grained Local Contrast** Since the alignment of the global view  $G$  with the text summarization  $T_S$  described above is relatively coarse, finer-grained information is largely discarded. Intuitively, image sub-regions can be aligned with some descriptions of the caption. To this end, we introduce fine-grained local contrast. We set the random cropping ratio for generating local view  $L$  to be  $[0.5, 1]$ , which focuses on the sub-region of the image  $I$ . The original caption  $T$  contains many detailed descriptions, so it is more suitable to be regarded as a pair of positive samples with  $L$ . Then the projected embeddings  $v^l$  and  $l^t$  of  $L$  and  $T$  are also brought together through contrastive loss (refer to Section 3.4).

### 3.3 Cross-level Relation Alignment

To further improve the alignment precision, we introduce the ROI feature sequence of salient objects in the image to provide more supervisions. Specifically, given an image  $I$  with  $M$  salient objects, we use a pre-trained object detector Faster R-CNN to extract the visual semantics of each object region as  $[\mathbf{o}'_m, \mathbf{z}_m]$ , where  $m$  denotes the  $m_{th}$  object,  $\mathbf{o}'_m$  is a 2048-dimensional feature vector and  $\mathbf{z}_m$  is a 4-dimensional normalized position vector indicating the coordinates of top-left and bottom-right corners. By concatenating  $\mathbf{o}'_m$  and  $\mathbf{z}_m$ , we have the 2052-dimensional position-sensitive ROI feature vector  $\mathbf{o}_m$ , forming the ROI feature sequence  $\mathcal{R} = \{\mathbf{o}_1, \mathbf{o}_2, \dots, \mathbf{o}_M\}$ . Then  $\mathcal{R} \in \mathbb{R}^{M \times 2052}$  is transformed into  $\mathbb{R}^{M \times d}$  using the projector in the embedding module  $\varphi$ , where  $d$  indicates the latent dimension of the MHSA layers in the image encoder. A randomly initialized  $d$ -dimensional class token is additionally appended at the front, resulting  $\mathcal{F} \in \mathbb{R}^{(1+M) \times d}$  which is further feed into the rear part  $f_2$  of the image encoder to compute the normalized ROI relation embedding  $\mathbf{v}^r$ , *i.e.*,  $\mathcal{F} = \varphi(\mathcal{R})$  and  $\mathbf{v}^r = f_2(\mathcal{F})$ . Note that feature sequence  $\mathcal{F}$  is position-sensitive following  $\mathcal{R}$ . Thus, positional embedding is not applied before it enters into the MHSA layer. To enhance the text encoder’s capability of modelling the relation of concepts, while avoiding weakening the reasoning ability of the visual encoder,  $(\mathbf{v}^r, \mathbf{l}^s)$  and  $(\mathbf{v}^r, \mathbf{l}^t)$  are used as another two positive pairs, and the distance between  $\mathbf{v}^r$  and  $\mathbf{l}^s$  and the distance between  $\mathbf{v}^r$  and  $\mathbf{l}^t$  are minimized simultaneously. Since the instance-level input used by the visual modality is very fine-grained, while the input employed by the linguistic modality is complete sentences (both text summarization and the original caption), we term this training process *cross-level relation alignment*.

In the case that the visual model is a convolution neural network (CNN), the traditional pooling layer is replaced by attention pooling, which actually is a MHSA layer. So the embedded ROI feature sequence  $\mathcal{F}$  is input to the attention pooling layer, *i.e.*,  $f_2$ , which indicates the final attention pooling layer, as shown in Figure 3(a). For the transformer-based visual model (ViT), the sequence  $\mathcal{F}$  can be directly input to a transformer layer. Considering that  $\mathcal{F}$  already encodes high-level visual semantics, we feed it into the rear part  $f_2$  of the ViT encoder, see Figure 3(b).



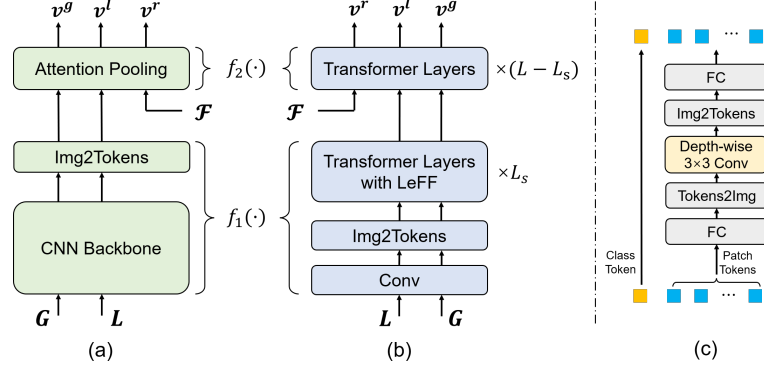


**Figure 3:** (a) The schematic of CNN-based image encoder. (b) The schematic of ViT-based image encoder. (c) The structure of LeFF module in ViT.

Besides, as pointed out in [22, 23], the standard ViT may not fully leverage the local context information, which limits the visual representation capacity of the ViT-based image encoder. Following [23], we incorporate a depth-wise convolution into the Feed-Forward module of the ViT architecture, termed Locally-enhanced Feed-Forward module (LeFF), improving the patch-level local perception and interaction. The structure of LeFF is shown in Figure 3(c). First, the patch tokens are projected into a higher dimension through a linear projection layer and reshaped. Next, a  $3 \times 3$  depth-wise convolution is utilized to capture the local information. Then the feature maps are flattened to a token sequence and re-projected into the initial dimension. While the class token is identical during the process and is concatenated with locally-enhanced patch tokens, generating the final output. As depicted in Figure 3(b), LeFF is only applied in the front part  $f_1$  of the ViT-based image encoder, since it is clearly not suitable for the embedded ROI feature sequence  $\mathcal{F}$ . In Figure 3(b),  $L$  denotes the total number of transformer layers in ViT and  $L_s$  is the number of transformer layers with LeFF in  $f_1$ . The influence of different settings of  $L_s$  can be seen in Section 4.5.

### 3.4 Softened Objective Function

For a batch of  $N$  image-text pairs  $\{(I_i, T_i)\}_{i=1}^N$ , where  $i$  indicates the  $i_{th}$  pair, the normalized embedded vectors  $\{v_i^g, v_i^l, v_i^r, l_i^s, l_i^t\}_{i=1}^N$  of the same dimension are obtained by the dual-stream encoders. In this formulation,  $v_i^g, v_i^l$ , and  $v_i^r$  are generated by the image encoder from global-crop image  $G$ , local-crop image  $L$  and ROI feature sequence  $\mathcal{R}$  respectively, while  $l_i^s, l_i^t$  are generated by the text encoder from the text summarization  $T_S$  and the original text  $T$  respectively. Then we use this vector group to construct four supervision signals  $\mathcal{L}_{GS}, \mathcal{L}_{LT}, \mathcal{L}_{RS}$  and  $\mathcal{L}_{RT}$  for in-batch contrastive learning, which can be calculated with  $\{(v_i^g, l_i^s)\}_{i=1}^N, \{(v_i^l, l_i^t)\}_{i=1}^N, \{(v_i^r, l_i^s)\}_{i=1}^N$  and  $\{(v_i^r, l_i^t)\}_{i=1}^N$  respectively. Our four contrastive losses, with the formulation of InfoNCE [24], are designed to achieve the alignment between visual representation and linguistic representation from disparate semantic levels.

Take the first loss term  $\mathcal{L}_{GS}$  from  $\{(v_i^g, l_i^s)\}_{i=1}^N$  as an example. For the  $i_{th}$  pair, the normalized vision-to-language similarity  $p_i^A(G) = \{p_{ij}^A(G)\}_{j=1}^N$  and language-to-vision similarity  $p_i^B(T_S) = \{p_{ij}^B(T_S)\}_{j=1}^N$  can be calculated through:

$$p_{ij}^A(G) = \frac{\exp(\text{sim}(v_i^g, l_j^s)/\tau)}{\sum_{j=1}^N \exp(\text{sim}(v_i^g, l_j^s)/\tau)}, \quad (1)$$

$$p_{ij}^B(T_S) = \frac{\exp(\text{sim}(l_i^s, v_j^g)/\tau)}{\sum_{j=1}^N \exp(\text{sim}(l_i^s, v_j^g)/\tau)}, \quad (2)$$

where  $\tau$  is a learnable temperature parameter initialized with 0.07 and the function  $\text{sim}(\cdot)$  conducts dot product to measure the similarity scores.

In standard practice, the corresponding label vectors of the ground-truth labels  $y_i^A(G) = \{y_{ij}^A(G)\}_{j=1}^N$  and  $y_i^B(T_S) = \{y_{ij}^B(T_S)\}_{j=1}^N$ , with positive pair denoted by 1 and negatives by 0, are used as the

targets to calculate cross-entropy. This kind of hard targets assumes there is absolutely no similarity between unpaired image and text. However, within a large-size batch, unpaired image and text may have more or less local similarity, *i.e.*, some local regions in the image may be matched with some words or phrases in other unpaired text. To address this problem for better generalization, we use label smoothing to soften the hard targets. The corresponding soften targets  $\tilde{\mathbf{y}}_i^A(G)$  and  $\tilde{\mathbf{y}}_i^B(T_S)$  for the  $i_{th}$  pair can be written as:

$$\tilde{\mathbf{y}}_i^A(G) = (1 - \alpha)\mathbf{y}_i^A(G) + \alpha/(N - 1), \quad (3)$$

$$\tilde{\mathbf{y}}_i^B(T_S) = (1 - \alpha)\mathbf{y}_i^B(T_S) + \alpha/(N - 1), \quad (4)$$

where  $\alpha$  is the smoothing hyper-parameter set to 0.2 in our experiments. Then the loss term  $\mathcal{L}_{GS}$  can be formulated as:

$$\mathcal{L}_{GS} = -\frac{1}{2N} \sum_{i=1}^N \sum_{j=1}^N (\tilde{\mathbf{y}}_{ij}^A(G) \cdot \log(p_{ij}^A(G)) + \tilde{\mathbf{y}}_{ij}^B(T_S) \cdot \log(p_{ij}^B(T_S))). \quad (5)$$

The other three loss terms  $\mathcal{L}_{LT}$ ,  $\mathcal{L}_{RS}$  and  $\mathcal{L}_{RT}$  can be calculated similarly. Therefore, the overall objective function of PyramidCLIP is

$$\mathcal{L} = (1 - \lambda - \mu - \gamma)\mathcal{L}_{GS} + \lambda\mathcal{L}_{LT} + \mu\mathcal{L}_{RS} + \gamma\mathcal{L}_{RT}, \quad (6)$$

where the loss weights  $\lambda$ ,  $\mu$  and  $\gamma$  are all set to 0.25 in our experiments.

## 4 Experiments

### 4.1 Datasets

**Pre-training Datasets** All the pre-training datasets that we used and the corresponding number of image-text pairs are listed in Table 1.

**Table 1:** Pre-training datasets.

Datasets	SBU	CC3M	CC12M	YFCC15M-V1	LAION99M	Total
#(Image, Text) Pair	1M	3M	10M	15M	99M	128M

SBU [25] is a relatively small image-text dataset, which contains 1 million image-text pairs obtained from Flickr. YFCC15M [12] is a commonly used subset of YFCC100M [12] and there are mainly two versions of YFCC15M, V1 and V2. YFCC15M-V1 is obtained by applying the same filtering rule on YFCC100M as CLIP [6], while YFCC15M-V2 is collected by DeCLIP [10] with a different filtering strategy. In addition to a subset of YFCC, the V2 dataset also contains some additional data crawled from the Internet and is of higher quality than V1. Note that YFCC15M-V1 is used in our experiments. CC3M [26] and CC12M [27] conduct the same image-text filter pipeline on Internet webpage sources, and the difference is that the filtering method of the latter is more relaxed. LAION400M [28] is currently one of the largest openly available image-text datasets. We rank the image-text pairs by their similarity scores, which are pre-computed by the producer using a pre-trained CLIP model, and pick up a 99M subset with the highest similarity scores. Combining all the above datasets, we finally have a dataset of 128M image-text pairs.

**Extraction of Text Summarization** We use the publicly released T5 model [20] to extract text summarization for all texts.

**Extraction of Object Region Features** We utilize the object detector Faster R-CNN pre-trained by VinVL [17] to extract salient object features in the image. Specifically, we resize the image to the size of  $640 \times 640$ , then input it into the detector, and take 10 objects with the highest confidence and extract the feature of each object from the ROI pooling layer of the detector.

**Downstream Datasets** We validate the effectiveness of our proposed method on three downstream tasks: the zero-shot image classification, zero-shot image-text retrieval and image object detection. For zero-shot image classification, experiments are carried out on ImageNet [14]. For the zero-shot image-text retrieval task, experiments are conducted on MS-COCO [29]. For the object detection task, the proposed method is verified on PASCAL VOC [30].

## 4.2 Implementation Details

**Pre-training Settings** We experiment on three different architectures, PyramidCLIP-ResNet50, PyramidCLIP-ViT-B/32 and PyramidCLIP-ViT-B/16, according to the choice of image encoder. Their detailed architecture designs follow that of CLIP [6]. The input resolution of image encoder is  $224 \times 224$  and the maximum context length of text encoder is 77. We train the three models using an AdamW [31] optimizer and the cosine learning rate schedule with a linear warmup. Specifically, the learning rate linearly increases from 0 to  $5 \times 10^{-4}$  within 10% of the total steps, and then decreases with a cosine anneal strategy. The weight decay rate of AdamW is set to 0.2. To save GPU memory, automatic mixed-precision [32] is used. We train PyramidCLIP from scratch for either 8 or 32 epochs in our experiments. Besides, the training batch size is set to 4096 on 15M dataset and 8192 on the large-scale dataset.

**Downstream Zero-shot Image Classification** Due to the fact that the labels of common classification datasets are mostly nouns rather than natural language descriptions, we follow the same prompt setting as used in CLIP, that is, for every single class name, we generate 80 different textual descriptions with 80 prompt templates (such as “a photo of label”). The ensembles of these textual representations are used in computing similarity between images and label names.

**Downstream Zero-shot Image-text Retrieval** The image-text retrieval task can be split into two sub-tasks, *i.e.*, image retrieval and text retrieval, according to the target modality. We evaluate the zero-shot image-text retrieval capabilities on the MS-COCO dataset, which is performed by ranking image-text pairs according to their similarity scores.

**Downstream Object Detection** Following [33, 34], for the downstream object detection task, we fine tune the whole model. The detector is trained for 24k steps with a batch size of 40, and the initial learning rate is 0.02 with 100 warm-up iterations and decays by 10 at 18k, 22k steps. The scale of image is randomly sampled from [480, 800] with interval 32 during the training and is set to 800 for inference.

## 4.3 Fair Comparison against SoTA

We first validate our method on the ImageNet zero-shot classification task and MS-COCO zero-shot image-text retrieval task using the same amount of pre-training data.

### 4.3.1 Comparison on YFCC15M

For fair comparison, we conduct experiments on YFCC15M-V1 and the results are shown in Table 2 and Table 3. It can be seen that our method significantly exceeds the results of CLIP baseline when both are pre-trained on YFCC15M-V1. In particular, as exhibited in Table 2, compared to the CLIP baseline, PyramidCLIP improves the ImageNet zero-shot top-1 accuracy by 19.2%/18.5%/19.6% when the visual model is ResNet50/ViT-B/32/ViT-B/16. Furthermore, PyramidCLIP exceeds DeFILIP by 5.0%, which is the combination of DeCLIP and FILIP, when the visual model is ViT-B/32. Note that we also list the results of other methods pre-trained on YFCC15M-V2 for reference. Since the quality of V2 is higher than that of V1, the results on V2 are better than those on V1, but our method still significantly exceeds them, showing the superiority of PyramidCLIP. Furthermore, the results on the image-text retrieval task in Table 3 also demonstrates the effectiveness of Pyramid.

**Table 2:** Zero-shot top1 accuracy on ImageNet. All the models are pre-trained for 32 epochs.

Method	Image Encoder	ImageNet ZS Top1
<i>Pre-trained on YFCC15M-V2</i>		
CLIP [6]	ResNet50	37.2 <sup>†</sup>
SLIP [35]	ResNet50	28.5 <sup>†</sup>
FILIP [8]	ResNet50	21.3 <sup>†</sup>
DECLIP [10]	ResNet50	41.9
CLIP [6]	ViT-B/32	32.8 <sup>†</sup>
SLIP[35]	ViT-B/32	34.3 <sup>†</sup>
<i>Pre-trained on YFCC15M-V1</i>		
CLIP <sup>◊</sup>	ResNet50	25.5
<b>PyramidCLIP</b>	ResNet50	<b>44.7</b>
CLIP <sup>◊</sup>	ViT-B/32	22.9
DeFILIP [36]	ViT-B/32	36.4 <sup>†</sup>
<b>PyramidCLIP</b>	ViT-B/32	<b>41.4</b>
CLIP <sup>◊</sup>	ViT-B/16	27.6
<b>PyramidCLIP</b>	ViT-B/16	<b>47.2</b>

◊ Our Implementation

† Reported in [36]



**Table 3:** Zero-shot image-text and text-image retrieval results on MS COCO. All the models are pre-trained for 32 epochs, except SLIP for 100 epochs.

Method	Image Encoder	MS COCO			
		I2T R@1	I2T R@5	T2I R@1	T2I R@5
<i>Pre-trained on YFCC15M-V1</i>					
CLIP <sup>◊</sup>	ResNet50	21.0	45.2	13.4	31.2
<b>PyramidCLIP</b>	ResNet50	<b>37.2</b>	<b>61.8</b>	<b>22.0</b>	<b>44.4</b>
CLIP <sup>◊</sup>	ViT-B/32	17.7	40.4	10.7	27.1
<b>PyramidCLIP</b>	ViT-B/32	<b>30.8</b>	<b>57.0</b>	<b>18.9</b>	<b>41.1</b>
SLIP [35]	ViT-B/16	33.9	60.0	22.5	45.4
CLIP <sup>◊</sup>	ViT-B/16	22.1	45.8	13.0	30.9
<b>PyramidCLIP</b>	ViT-B/16	<b>34.7</b>	<b>61.6</b>	<b>22.7</b>	<b>45.5</b>

<sup>◊</sup> Our Implementation

#### 4.3.2 Comparison on LAION15M

Since the distribution of different datasets can vary vastly, we not only conduct experiments on the commonly used YFCC15M dataset, but also sample 15 millions image-text pairs from LAION400M for fair comparison. The results are shown in Table 4, it can be seen that PyramidCLIP still outperforms the CLIP baseline by a large margin, regardless of the visual encoder used.

**Table 4:** Zero-shot image-text and text-image retrieval results on MS COCO and zero-shot top1 accuracy on ImageNet. All the models are pre-trained on LAION15M for 32 epochs.

Method	Image Encoder	MS COCO				ImageNet
		I2T R@1	I2T R@5	T2I R@1	T2I R@5	ZS Top1
CLIP <sup>◊</sup>	ResNet50	<b>31.5</b>	57.0	18.9	39.8	35.6
<b>PyramidCLIP</b>	ResNet50	31.2	<b>57.7</b>	<b>21.4</b>	<b>44.5</b>	<b>41.1</b>
CLIP <sup>◊</sup>	ViT-B/32	<b>25.9</b>	49.8	15.6	34.8	32.6
<b>PyramidCLIP</b>	ViT-B/32	25.3	<b>50.8</b>	<b>18.8</b>	<b>39.9</b>	<b>39.2</b>
CLIP <sup>◊</sup>	ViT-B/16	<b>31.4</b>	56.2	19.2	40.6	38.3
<b>PyramidCLIP</b>	ViT-B/16	30.6	<b>57.3</b>	<b>22.7</b>	<b>45.8</b>	<b>45.0</b>

<sup>◊</sup> Our Implementation

#### 4.4 Comparison on Large-scale Datasets

In this section, we validate the effectiveness of our method on a larger dataset, *i.e.* 128M image-text pairs, and the ImageNet zero-shot classification accuracy results are shown in Table 5. Due to the time and computational resource constraints, PyramidCLIP is only pre-trained for 8 epochs. With the same amount of pre-training data and the number of training epochs, PyramidCLIP significantly exceeds the results of the CLIP baseline by 4.7% and 6.8% using ResNet50 and ViT-B/32 as the image encoder, respectively. Furthermore, when the vision model is ResNet50, the result of PyramidCLIP only trained on 128M data for 8 epochs are already very close to that of CLIP trained on 400M data for 32 epochs.

#### 4.5 Ablation Study

In this section, we further explore the impact of each component in PyramidCLIP. Due to the time and resource constraints, all the ablation experiments are pre-trained for 8 epochs on YFCC15M-V1, and then transfer to the downstream zero-shot ImageNet classification task.

**The Influence of Different  $L_s$  Settings** We first explore the influence of the transformer layers  $L_s$  in the front part of ViT-

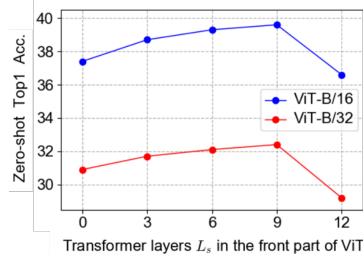


**Figure 4:** Zero-shot performance with different settings of  $L_s$ .

**Table 5:** Zero-shot top1 accuracy on ImageNet. All models are pre-trained on large-scale dataset.

Method	Image Encoder	Pre-training Setting		ImageNet ZS Top1
		# (Image, Text) Pair	Epoch	
CLIP [6]	ResNet50	400M	32	59.6
DECLIP [10]	ResNet50	88M	32	62.5
CLIP <sup>◊</sup>	ResNet50	128M	8	53.0
<b>PyramidCLIP</b>	ResNet50	128M	8	<b>57.7(+4.7)</b>
CLIP [6]	ViT-B/32	400M	32	63.2
DECLIP [10]	ViT-B/32	88M	32	66.2
FILIP [8]	ViT-B/32	340M	30	68.8
CLIP <sup>◊</sup>	ViT-B/32	128M	32	55.5
CLIP <sup>◊</sup>	ViT-B/32	128M	8	49.7
<b>PyramidCLIP</b>	ViT-B/32	128M	8	<b>56.5(+6.8)</b>
CLIP [6]	ViT-B/16	400M	32	68.6
CLIP <sup>◊</sup>	ViT-B/16	128M	8	54.4
<b>PyramidCLIP</b>	ViT-B/16	128M	8	<b>62.4(+8.0)</b>

<sup>◊</sup> Our Implementation

based image encoder. Note that the total number of transformer layers  $L$  in ViT is 12. The corresponding results with different  $L_s$  values are shown in Figure 4. It can be found that setting  $L_s$  to 9 achieves the best result, hence  $L_s = 9$  in our experiments. Besides,  $L_s = 0$  represents that the feature sequence  $\mathcal{F}$  is input to the first transformer layer of ViT and all the layers are without using LeFF. While  $L_s = 12$  indicates that all the 12 layers are with LeFF and the raw sequence  $\mathcal{F}$  is directly input to the final projector without being processed by transformer, which is the reason why  $L_s = 12$  shows such poor performance.

**The Effectiveness of Each Component** We further verify the effectiveness of each component in PyramidCLIP and the results are shown in Table 6. It is worth noting that  $\mathcal{L}_{\text{CLIP}}$  represents the original CLIP loss, which is actually the contrastive loss between the image global view and the original text. Obviously  $\mathcal{L}_{\text{LT}}$  performs better than  $\mathcal{L}_{\text{CLIP}}$ , since the local view statistically removes some unimportant information in the image, *i.e.*, some sub-regions not described in the text. This is why we use the image local view and the original text to construct the local contrastive loss. Besides, it can also be seen that other components, including  $\mathcal{L}_{\text{GS}}$ ,  $\mathcal{L}_{\text{RT}}$ ,  $\mathcal{L}_{\text{RS}}$ , LeFF of ViT and soften objectives in PyramidCLIP, can all bring significant gains individually.

**Table 6:** Ablation study of each component on ImageNet zero-shot classification task.  $\mathcal{L}_{\text{CLIP}}$  represents the original CLIP loss. “LeFF” represents the operation of incorporating depth-wise convolution into the FFN layer of ViT. “Soften” means that all the objectives are softened.

Image Encoder	Components							ImageNet	
	$\mathcal{L}_{\text{CLIP}}$	$\mathcal{L}_{\text{LT}}$	$\mathcal{L}_{\text{GS}}$	LeFF	$\mathcal{L}_{\text{RT}}$	$\mathcal{L}_{\text{RS}}$	Soften	ZS Top1	ZS Top5
ResNet50	✓			-				29.2	53.6
		✓		-				30.3(+1.1)	54.8(+1.2)
		✓	✓	-				34.7(+5.5)	60.6(+7.0)
		✓	✓	-	✓			35.9(+6.7)	63.1(+9.5)
		✓	✓	-	✓	✓		37.2(+8.0)	63.9(+10.3)
		✓	✓	-	✓	✓	✓	<b>38.5(+9.3)</b>	<b>64.7(+11.1)</b>
ViT-B/16	✓							25.6	49.0
		✓						27.3(+1.7)	50.7(+1.7)
		✓	✓					33.4(+7.8)	58.5(+9.5)
		✓	✓	✓				36.0(+10.4)	61.7(+12.7)
		✓	✓	✓	✓			38.6(+13.0)	65.2(+16.2)
		✓	✓	✓	✓	✓		39.6(+14.0)	66.1(+17.1)
		✓	✓	✓	✓	✓	✓	<b>41.3(+15.7)</b>	<b>68.1(+19.1)</b>

#### 4.6 Downstream Task: Object Detection

In order to verify that our model can better exploit the relationship between objects in the image, we validate our models on the object detection task. Specifically, we take the visual model ResNet50 and then use it as the backbone of C4 based Faster R-CNN. The results are shown in the Table 7. It can be seen that compared against the CLIP baseline, our method performs better both for the cases that it is pre-trained on YFCC15M and LAION15M, and it is more significant on YFCC15M. Furthermore, the penultimate line denotes that PyramidCLIP only adopts semantics contrastive loss without using the relations, and it can be seen that cross-level relation contrast brings more improvement in detection than intra-level semantics contrast, indicating the relation contrast can indeed enhance the relation reasoning ability of visual models, which is expected.

**Table 7:** Object detection results on the VOC07 test with ResNet-50 backbone C4 based Faster R-CNN.

Method	Pre-training Dataset	PASCAL VOC		
		$AP^{bb}$	$AP_{50}^{bb}$	$AP_{75}^{bb}$
<i>Comparison against CLIP, 32ep</i>				
CLIP <sup>◇</sup>	YFCC15M	45.0	72.7	46.6
<b>PyramidCLIP</b>	YFCC15M	<b>49.2(+4.2)</b>	<b>77.1(+4.4)</b>	<b>52.5(+5.9)</b>
CLIP <sup>◇</sup>	LAION15M	46.8	74.9	49.5
<b>PyramidCLIP</b>	LAION15M	<b>48.6(+1.8)</b>	<b>76.4(+1.5)</b>	<b>52.5(+3.0)</b>
<i>Ablation on YFCC15M, 8ep</i>				
CLIP <sup>◇</sup>	YFCC15M	43.5	72.4	45.3
<b>PyramidCLIP (w/o Relation)</b>	YFCC15M	45.2(+1.7)	74.1(+1.7)	46.9(+1.6)
<b>PyramidCLIP</b>	YFCC15M	<b>46.8(+3.3)</b>	<b>75.6(+3.2)</b>	<b>49.8(+4.5)</b>

<sup>◇</sup> Our Implementation

## 5 Conclusion

In this paper, we have proposed a hierarchical pre-training method, termed PyramidCLIP, to achieve improved alignment between visual and linguistic modalities. It resolves the issue that the webly-crawled data is not in perfect one-to-one correspondence by explicitly constructing pyramidal semantic inputs at the both sides of dual-stream network. We also show that softened intra-level semantics alignment and cross-level relation alignment can interact between two modalities and are beneficial. PyramidCLIP achieves the state-of-the-art results on three downstream tasks, which demonstrates the superiority.

## References

- [1] Y.-C. Chen, L. Li, L. Yu, A. El Kholy, F. Ahmed, Z. Gan, Y. Cheng, and J. Liu, “Uniter: Universal image-text representation learning,” in *Proc. European Conf. Computer Vision*, 2020, pp. 104–120.
- [2] L. H. Li, M. Yatskar, D. Yin, C.-J. Hsieh, and K.-W. Chang, “Visualbert: A simple and performant baseline for vision and language,” *arXiv preprint arXiv:1908.03557*, 2019.
- [3] X. Li, X. Yin, C. Li, P. Zhang, X. Hu, L. Zhang, L. Wang, H. Hu, L. Dong, F. Wei *et al.*, “Oscar: Object-semantics aligned pre-training for vision-language tasks,” in *Proc. European Conf. Computer Vision*, 2020, pp. 121–137.
- [4] G. Li, N. Duan, Y. Fang, M. Gong, and D. Jiang, “Unicoder-vl: A universal encoder for vision and language by cross-modal pre-training,” in *Proceedings of the AAAI Conference on Artificial Intelligence*, vol. 34, no. 07, 2020, pp. 11 336–11 344.
- [5] W. Su, X. Zhu, Y. Cao, B. Li, L. Lu, F. Wei, and J. Dai, “Vi-bert: Pre-training of generic visual-linguistic representations,” *arXiv preprint arXiv:1908.08530*, 2019.
- [6] A. Radford, J. W. Kim, C. Hallacy, A. Ramesh, G. Goh, S. Agarwal, G. Sastry, A. Askell, P. Mishkin, J. Clark *et al.*, “Learning transferable visual models from natural language supervision,” in *Proc. International Conf. Machine Learning*, 2021, pp. 8748–8763.

- [7] C. Jia, Y. Yang, Y. Xia, Y.-T. Chen, Z. Parekh, H. Pham, Q. Le, Y.-H. Sung, Z. Li, and T. Duerig, “Scaling up visual and vision-language representation learning with noisy text supervision,” in *International Conference on Machine Learning*. PMLR, 2021, pp. 4904–4916.
- [8] L. Yao, R. Huang, L. Hou, G. Lu, M. Niu, H. Xu, X. Liang, Z. Li, X. Jiang, and C. Xu, “Filip: Fine-grained interactive language-image pre-training,” *arXiv preprint arXiv:2111.07783*, 2021.
- [9] H. Tan and M. Bansal, “Lxmert: Learning cross-modality encoder representations from transformers,” *arXiv preprint arXiv:1908.07490*, 2019.
- [10] Y. Li, F. Liang, L. Zhao, Y. Cui, W. Ouyang, J. Shao, F. Yu, and J. Yan, “Supervision exists everywhere: A data efficient contrastive language-image pre-training paradigm,” *arXiv preprint arXiv:2110.05208*, 2021.
- [11] A. Dosovitskiy, L. Beyer, A. Kolesnikov, D. Weissenborn, X. Zhai, T. Unterthiner, M. Dehghani, M. Minderer, G. Heigold, S. Gelly *et al.*, “An image is worth 16x16 words: Transformers for image recognition at scale,” *arXiv preprint arXiv:2010.11929*, 2020.
- [12] B. Thomee, D. A. Shamma, G. Friedland, B. Elizalde, K. Ni, D. Poland, D. Borth, and L.-J. Li, “Yfcc100m: The new data in multimedia research,” *Communications of the ACM*, vol. 59, no. 2, pp. 64–73, 2016.
- [13] K. He, X. Zhang, S. Ren, and J. Sun, “Deep residual learning for image recognition,” in *Proc. IEEE Conf. Computer Vision and Pattern Recognition*, 2016, pp. 770–778.
- [14] J. Deng, W. Dong, R. Socher, L.-J. Li, K. Li, and L. Fei-Fei, “Imagenet: A large-scale hierarchical image database,” in *Proc. IEEE Conf. Computer Vision and Pattern Recognition*, 2009, pp. 248–255.
- [15] W. Li, C. Gao, G. Niu, X. Xiao, H. Liu, J. Liu, H. Wu, and H. Wang, “Unimo: Towards unified-modal understanding and generation via cross-modal contrastive learning,” *arXiv preprint arXiv:2012.15409*, 2020.
- [16] J. Lu, D. Batra, D. Parikh, and S. Lee, “Vilbert: Pretraining task-agnostic visiolinguistic representations for vision-and-language tasks,” *Proc. Advances in Neural Information Processing Systems*, vol. 32, 2019.
- [17] P. Zhang, X. Li, X. Hu, J. Yang, L. Zhang, L. Wang, Y. Choi, and J. Gao, “Vinvl: Revisiting visual representations in vision-language models,” in *Proc. IEEE/CVF Conf. Computer Vision & Pattern Recognition*, 2021, pp. 5579–5588.
- [18] Z. Li, Z. Fan, H. Tou, Z. Wei, and X. Huang, “Mvptr: Multi-stage vision-language pre-training via multi-level semantic alignment,” *arXiv preprint arXiv:2201.12596*, 2022.
- [19] Y. Zeng, X. Zhang, and H. Li, “Multi-grained vision language pre-training: Aligning texts with visual concepts,” *arXiv preprint arXiv:2111.08276*, 2021.
- [20] C. Raffel, N. Shazeer, A. Roberts, K. Lee, S. Narang, M. Matena, Y. Zhou, W. Li, and P. J. Liu, “Exploring the limits of transfer learning with a unified text-to-text transformer,” *arXiv preprint arXiv:1910.10683*, 2019.
- [21] S. Ren, K. He, R. Girshick, and J. Sun, “Faster R-CNN: Towards real-time object detection with region proposal networks,” *Proc. Advances in Neural Information Processing Systems*, vol. 28, 2015.
- [22] J. Guo, K. Han, H. Wu, C. Xu, Y. Tang, C. Xu, and Y. Wang, “Cmt: Convolutional neural networks meet vision transformers,” *arXiv preprint arXiv:2107.06263*, 2021.
- [23] K. Yuan, S. Guo, Z. Liu, A. Zhou, F. Yu, and W. Wu, “Incorporating convolution designs into visual transformers,” in *Proceedings of the IEEE/CVF International Conference on Computer Vision*, 2021, pp. 579–588.
- [24] A. Van den Oord, Y. Li, O. Vinyals *et al.*, “Representation learning with contrastive predictive coding,” *arXiv preprint arXiv:1807.03748*, vol. 2, no. 3, p. 4, 2018.
- [25] V. Ordonez, G. Kulkarni, and T. Berg, “Im2text: Describing images using 1 million captioned photographs,” *Proc. Advances in Neural Information Processing Systems*, vol. 24, 2011.
- [26] P. Sharma, N. Ding, S. Goodman, and R. Soicrut, “Conceptual captions: A cleaned, hypernymed, image alt-text dataset for automatic image captioning,” in *Proceedings of the 56th Annual Meeting of the Association for Computational Linguistics (Volume 1: Long Papers)*, 2018, pp. 2556–2565.
- [27] S. Changpinyo, P. Sharma, N. Ding, and R. Soicrut, “Conceptual 12m: Pushing web-scale image-text pre-training to recognize long-tail visual concepts,” in *Proceedings of the IEEE/CVF Conference on Computer Vision and Pattern Recognition*, 2021, pp. 3558–3568.
- [28] C. Schuhmann, R. Vencu, R. Beaumont, R. Kaczmarczyk, C. Mullis, A. Katta, T. Coombes, J. Jitsev, and A. Komatsuzaki, “Laion-400m: Open dataset of clip-filtered 400 million image-text pairs,” *arXiv preprint arXiv:2111.02114*, 2021.
- [29] T.-Y. Lin, M. Maire, S. Belongie, J. Hays, P. Perona, D. Ramanan, P. Dollár, and C. L. Zitnick, “Microsoft coco: Common objects in context,” in *Proc. European Conf. Computer Vision*, 2014, pp. 740–755.

- [30] M. Everingham, S. Eslami, L. Van Gool, C. K. Williams, J. Winn, and A. Zisserman, “The pascal visual object classes challenge: A retrospective,” *International journal of computer vision*, vol. 111, no. 1, pp. 98–136, 2015.
- [31] I. Loshchilov and F. Hutter, “Decoupled weight decay regularization,” *arXiv preprint arXiv:1711.05101*, 2017.
- [32] P. Micikevicius, S. Narang, J. Alben, G. Diamos, E. Elsen, D. Garcia, B. Ginsburg, M. Houston, O. Kuchaiev, G. Venkatesh, and H. Wu, “Mixed precision training,” in *International Conference on Learning Representations*, 2018.
- [33] Z. Fang, J. Wang, L. Wang, L. Zhang, Y. Yang, and Z. Liu, “Seed: Self-supervised distillation for visual representation,” *arXiv preprint arXiv:2101.04731*, 2021.
- [34] Y. Gao, J.-X. Zhuang, K. Li, H. Cheng, X. Guo, F. Huang, R. Ji, and X. Sun, “Disco: Remedy self-supervised learning on lightweight models with distilled contrastive learning,” *arXiv preprint arXiv:2104.09124*, 2021.
- [35] N. Mu, A. Kirillov, D. Wagner, and S. Xie, “Slip: Self-supervision meets language-image pre-training,” *arXiv preprint arXiv:2112.12750*, 2021.
- [36] Y. Cui, L. Zhao, F. Liang, Y. Li, and J. Shao, “Democratizing contrastive language-image pre-training: A clip benchmark of data, model, and supervision,” *arXiv preprint arXiv:2203.05796*, 2022.